Available online at www.sciencedirect.com
SCIENCE DIRECT®
Carbohydrate Research 339 (2004) 251–258
Carbohydrate RESEARCH

Rod-like architecture and helicity of the poly(C)/schizophyllan complex observed by AFM and SEM ☆

Ah-Hyun Bae,[a] Seung-Woo Lee,[b] Masato Ikeda,[a] Masahito Sano,[c] Seiji Shinkai[a] and Kazuo Sakurai[b,*]

[a]*Department of Chemistry and Biochemistry, Graduate School of Engineering, Kyushu University, Fukuoka 812-8581, Japan*
[b]*Department of Chemical Processes and Environments, Faculty of Environmental Engineering, The University of Kitakyushu, Sakurai Laboratory, 1-1 Hibikino, Wakamatsu-ku, Kitakyushu-shi, Fukuoka-ken 808-0135, Japan*
[c]*Department of Polymer Science and Engineering, Yamahata University, Yonezawa 992-8510, Japan*

Received 27 May 2003; accepted 23 September 2003

Abstract—Microscopic studies of the complex between poly(C) and schizophyllan (SPG), employing both AFM and SEM, revealed that the complex takes the same rod-like architecture on the mica surface as those of the renatured SPG and the original triple helix of SPG, indicating that the complex also has a helical structure. The SEM observations showed the helical pattern on the rod surface, only when the sample was metal shadowed. The pitch evaluated from the image is comparable with that obtained from crystallographic data. The ability to visualize the helical structure can be explained from the hypothesis that the platinum grains may assemble on the sample using the molecular surface of the SPG (or complex) as the template.

Keywords: AFM; SEM; Schizophyllan; Poly(C); Complex; Rod-like architecture; Helicity

1. Introduction

Schizophyllan is a cell-wall polysaccharide produced by the fungus *Schizophyllum commune*. The main chain consists of β-(1→3)-D-glucan with one β-(1→6)-D-glucosyl side chain linked to the main chain at every three glucose residues (see Fig. 1a).[2] Norisuye and co-workers[3,4] showed that schizophyllan adopts a triple helical conformation (see Fig. 1b) in water and a random coil in dimethyl sulfoxide (Me_2SO). When water is added to the Me_2SO solution (renaturation), the single chain of schizophyllan (s-SPG) collapses owing to formation of hydrogen bonds.[5] McIntire and Brant[6] and Young and Dong[7] independently showed that the triple helical structure can be retrieved when the renaturation process is carried out in considerably dilute solutions (ca. 4–30 μg/mL). Recently, Sakurai and Shinkai[1,8–10] found that s-SPG forms a macromolecular complex with poly(C) when the polynucleotide is present in the renaturation process. They found that the complexation proceeds in a highly stoichiometric manner that is to say, two schizophyllan repeating units and three poly(C) units are bound in the complex.[9] This stoichiometric number can be interpreted in terms of two SPG chains and one poly(C) chain forming a new triple helix structure.[9,10]

According to X-ray crystallographic studies,[11–13] the triple helical schizophyllan (t-SPG) and the single chain of poly(C) form a right handed 6_1 triple helix with a 1.8 nm pitch and a right handed 6_1 helix with a 1.86 nm pitch, respectively. Since both helix parameters are surprisingly similar, we can assume that the helix formation from poly(C) and s-SPG chains may not induce either a large conformational change or an unfavorable entropy gain. If an enthalpy driving force (such as charge transfer or hydrogen bonding) is present between

☆ Polysaccharide–polynucleotide complexes,[1] Part 18.

* Corresponding author. Tel.: +81-93-695-3294; fax: +81-93-695-3298; e-mail addresses: sakurai@env.kitakyushu-u.ac.jp, sakurai@env.kitakyu-u.ac.jp

0008-6215/$ - see front matter © 2003 Elsevier Ltd. All rights reserved.
doi:10.1016/j.carres.2003.09.032

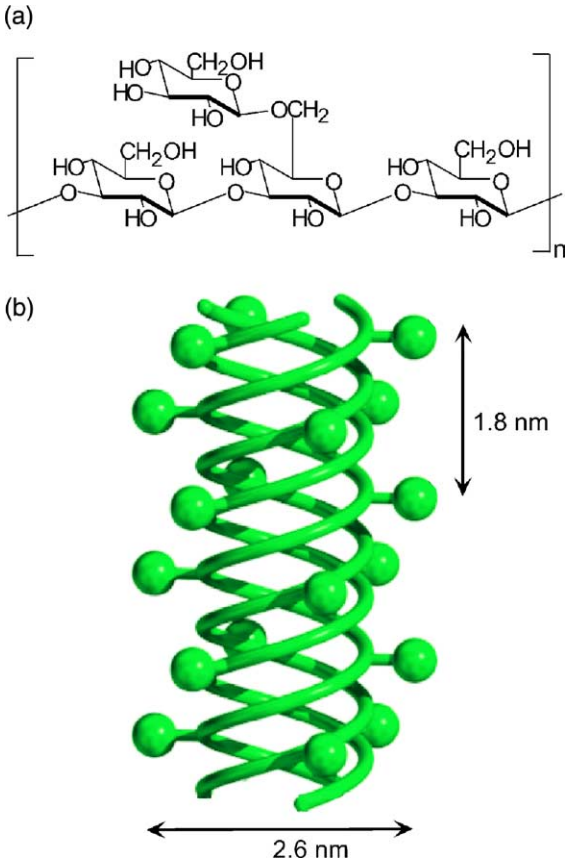

Figure 1. Repeating unit of schizophyllan (a) and a representative model of the triple helix (b); the balls represent the side chains.

poly(C) and s-SPG, two different chains can form a helical complex. In fact, our previous work[9] showed that the hydrogen-bonding interaction plays an important role in the complexation. Using the Discover 3 program, we took out one glucan chain from t-SPG and tried to fit one poly(C) chain into the groove occupied by the absent glucan.[10] We found that replacing one glucan chain by the poly(C) chain can be achieved easily without inducing significant steric hindrance. After replacing the glucan chain with poly(C), the most stable conformation for poly(C) in the groove was determined by molecular mechanics using the Amber force field, and the resultant structure is shown in Figure 2.[10] The glucan chains are presented by the CPK model and the poly(C) chain by a ball-and-stick model. As shown in the figure, the ribose takes 3′-endo conformation and the fourth amino group in the cytosine comes close enough to the second oxygen in s-SPG to form a hydrogen bond. All the above results are consistent with the speculation that the poly(C)/s-SPG complex forms a triple helix and that the helix parameter is similar to that of t-SPG. However, all of these results are still circumstantial evidence. The purpose of this paper is to present more direct visual evidence on the nature of the molecular complex.

Microscopic observation of biomolecules is a challenging issue,[14,15] and much work has been dedicated toward observation of the double helix of DNA.[15–17] Only a few papers have so far suggested that true helicity of the DNA structure can be seen with atomic force microscopy (AFM).[15,16] The difficulty is caused by the fact that the radius of the tips are generally larger than the pitch of the helix, and that the structure of the molecules is generally fairly flexible, and probably distorted by the imaging process. There are a considerable number of rod-like polysaccharides that have been imaged by AFM, including xanthan,[18] acetan,[19] gellan,[20] amylose,[21] and carrageenans.[21] However, due to the imperfect tip reading and the distorted image, there are only a few studies on acetan that show helical repeats consistent with that of X-ray diffraction data.[19] McIntire and Brant[6] and Stokke et al.[22] independently observed three β-(1 → 3)-D-glucans (scleroglucan, schizophyllan, and lentinan) with AFM and found that the natural glucans exhibit a rod-like architecture, which is expected from the studies on the dilute solution properties of those polymers. They also showed that the renatured materials may appear as macrocycles, depending on the

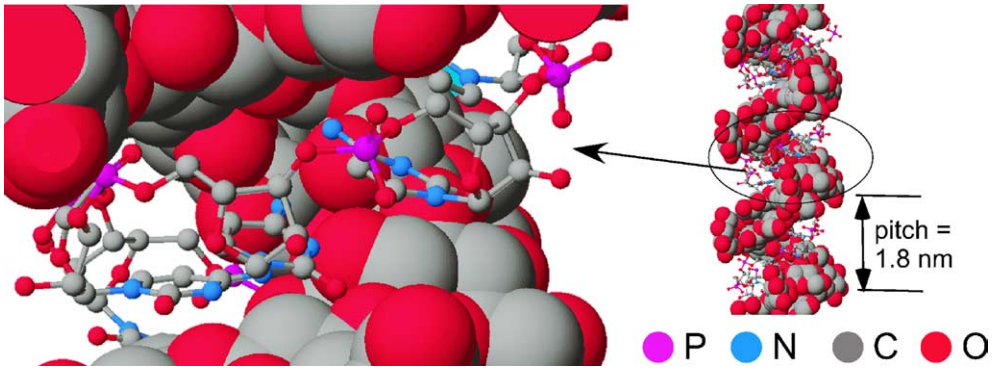

Figure 2. The most stable structure for the poly(C)/s-SPG complex obtained by molecular mechanics calculations. The glucan chains are presented by the CPK model and the poly(C) chain by a ball-and-stick model.

renaturing conditions.[6] However, the resolution was not good enough to observe the helicity of these polysaccharides. Kunitake and Ohira[23] used AFM to observe the conformation of schizophyllan. They reported some helical pattern on the molecule; however, the observed helicity was not consistent with the crystallographic data.

If the speculation that the complex forms a novel triple helix is valid, then we should be able to see a rod-like architecture for the complex. In this work, using both AFM and scanning electron microscopy (SEM), we have imaged the molecular architecture of the poly(C)/schizophyllan complex and compared it with that seen for renatured schizophyllan.

2. Results and discussion

2.1. AFM observation and rod-like architecture of the complex

Figure 3 compares the AFM images obtained when the s-SPG/poly(C) molar ratio is varied from 0 to 1.0. When the ratio is 1.0:0 (only renatured s-SPG, Panel 1), the image shows a mixture of rods and rings. Although the results are not presented, the image for t-SPG showed only rods with a similar length to that of the rods in Panel 1. The height of each rod or ring is about 2–3 nm, being consistent with that for the schizophyllan triple helix. The data shown in Panel 1 is consistent with that in reported studies for the renatured s-SPG samples.[6,18,22] All the experimental facts indicate that the rod represents the molecule, namely, a triple helix has been made from s-SPG in the renaturation process. We measured the contour length of the rods (L) in this panel as well as other AFM images taken under the same conditions, and plotted the results as the distribution of L in Figure 4B. For comparison, the distribution of L for t-SPG is presented in Figure 4A.

Using the gamma distribution (see the Experimental section), we evaluated the most suitable parameters to provide the matched distribution for the data, and the result is presented by the solid line. For both t-SPG and s-SPG, the data points are well fitted by a standard gamma distribution with $\alpha = 4.4$ (when $x = L/40$). Table 1 summarizes the number average L and the number-average molecular weight (M_n) and the weight-average molecular weight (M_w). All the statistical data for the renatured s-SPG agree with those of the original triple helix, indicating that the rod-like images in Panel 1 represent individual molecules, and the molecules have an equivalent molecular weight and distribution to those of the original triple helix. This fact evidences that the renaturation occurred via three individual s-SPG chains. Both M_n and M_w listed in the table are approximately 20% larger than those determined from gel-permeation chromatography (see the Experimental section). This discrepancy may be ascribed to an experimental error due to different technique, or suggests that we could not omit the aggregates completely when we measured L. There is a minor second maximum (or deviation from the gamma distribution) in the range of 300–400 nm. The origin of this maximum may be the molecular aggregates. There are some rings observed in Panel 1 as minor species. As has previously been pointed out,[6] these images are probably made from one or two s-SPG chains due to ring closure. When we measured the length of the molecules, we omitted these rings.

Panel 5 in Figure 3 shows the image obtained for poly(C). This consists of only circular dots, which seems typical for flexible chains.[24] Therefore, we can consider that the circular dots represent poly(C) molecules that are not involved in complexation with s-SPG. When we observed three mixtures of poly(C) and s-SPG (Panels 2–4), the rod population decreased and the dot population increased with increasing the poly(C) composition. However, even for the stoichiometric mixture (Panel 3), dots are observed. Hence the question needs to be asked whether the rod in the mixture represents the poly(C)/s-SPG complex or simply renatured s-SPG. In Panel 2 [the ratio = 4.5:1.0, the poly(C) composition is less than stoichiometric], there are no dots, suggesting that most poly(C) molecules are incorporated into the rods due to the complexation. Furthermore, rings in Panels 3 and 4 were less abundant than in the renatured s-SPG (Panel 1). The mixing of poly(C) and s-SPG was carried out in a nonsalt aqueous solution. Therefore, if the complex is formed, the electrostatic repulsion between the phosphate anions in poly(C) might hinder ring closure reactions. Although these features are consistent with complex formation, this evidence is not sufficient to prove that the rods represent complexes.

Measurements of L were made for the rods in Panel 4, as well as for the other AFM images taken under the same conditions. Figure 4C shows the distribution. By comparing this histogram with the others (t-SPG and s-SPG), it can be seen that the mixture has a different length distribution to those of the renatured s-SPG and t-SPG, indicating that the mixture has longer rods than the renatured s-SPG. This difference supports the suggestion that the presence of poly(C) influences the rod length through complexation. It is interesting that the mixture has a second maximum about the 300–350 nm length. Since poly(C) has 570 bases, the extended poly(C) chain is about 200 nm long, and that of s-SPG is about 180 nm long. Therefore, the second maximum around 300–350 nm can appear only when more than two s-SPG chains are involved in the complexation, as illustrated in the figure.

In order to fit the data for the mixture, we have to assume multiple distributions. In this work, we assumed two gamma functions; the first function is the same as that for the s-SPG, and the second one is a gamma

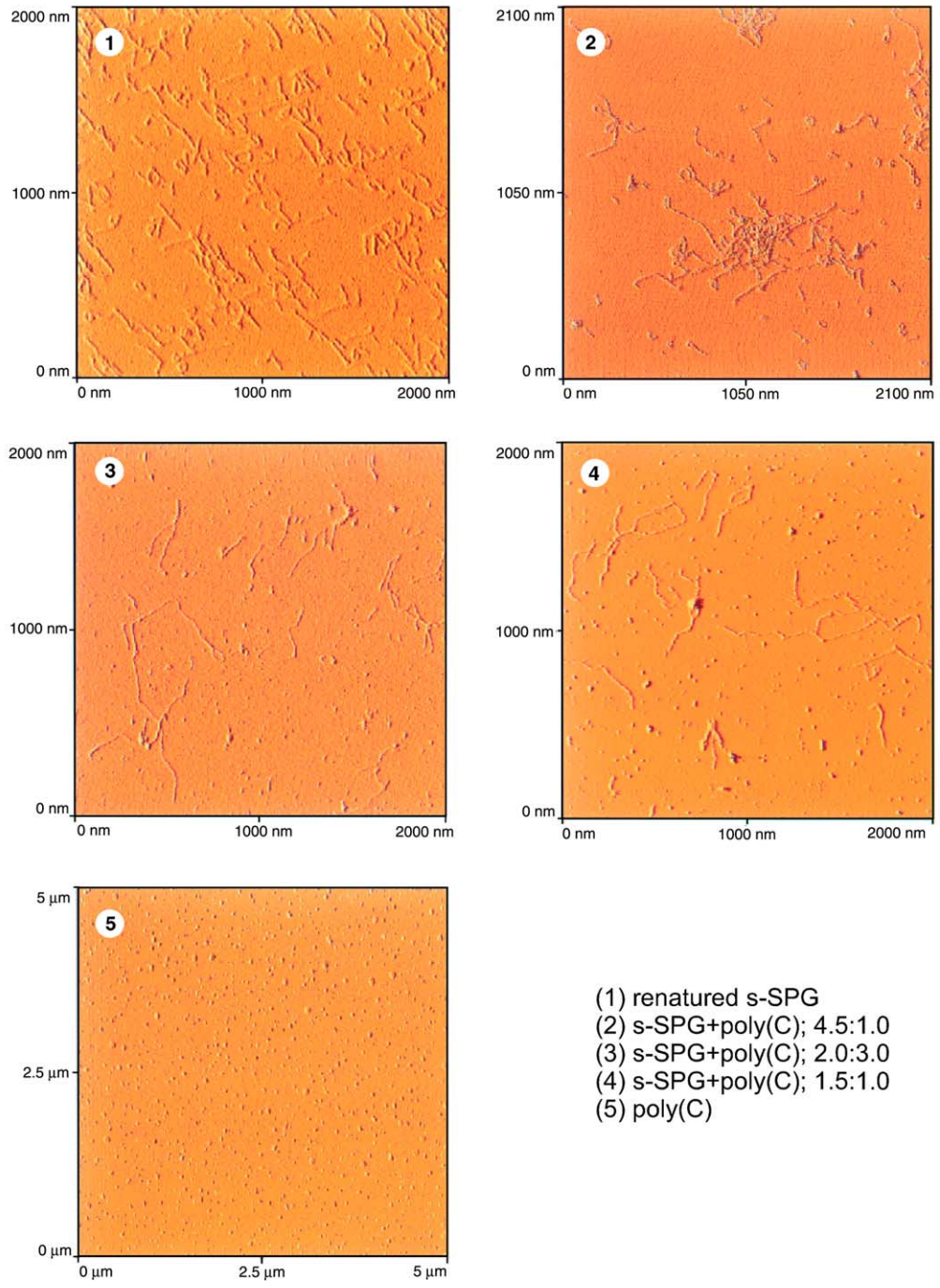

Figure 3. Comparison of the AFM images obtained when the s-SPG/poly(C) ratios are 1.0:0 (1), 4.5:1.0 (2), 2.0:3.0 (3), 1.5:1.0 (4), and 0:1.0 (5).

function with $\alpha = 4.4$ and $\beta = 1.0$. By iterating, we reached the conclusion that the measured distribution consists of 80% of the first one and 20% of the second. As a matter of fact, the second function can be any function such as the Poisson distribution. The important conclusion is that the mixture has a different length distribution from those of the renatured s-SPG and t-SPG, and 20% of the rods are almost twice as lon g as the original SPG. Furthermore, the complex exhibits a very long rods with $L > 500$ nm. This may be due to three helixes being connected with poly(C), as depicted in the figure.

2.2. SEM observation and the metal-grain array reflecting the molecular helicity

Figure 5 shows a typical SEM image for t-SPG. The thickness of the platinum coating (estimated from the coating time and current) is 16 nm, and the average size (diameter) of the rod-like image (d_t) is 20 ± 2 nm.

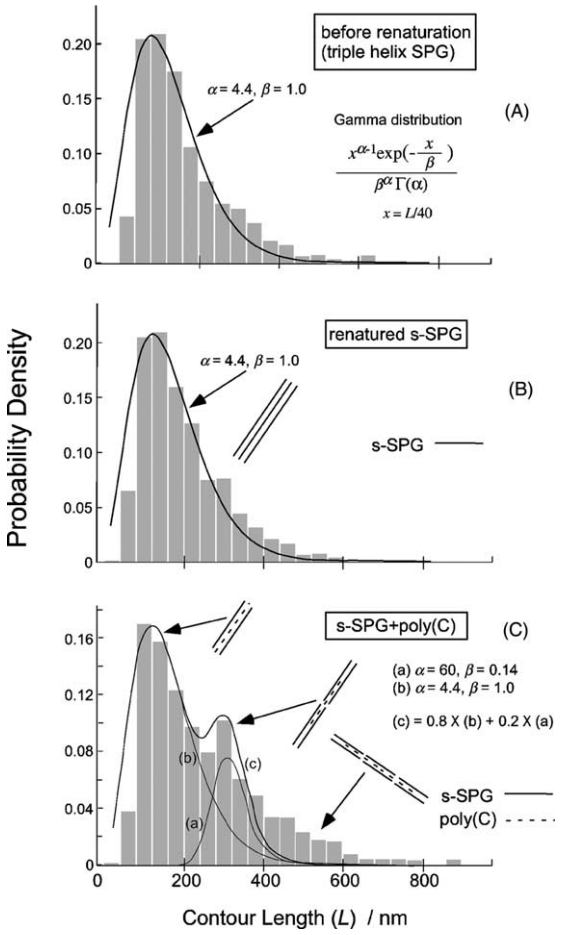

Figure 4. Comparison of the rod length distribution among the original triple helix (A), the renatured s-SPG (B) and the poly(C)/s-SPG mixture (C). The solid lines in (A) and (B) represent the standard gamma function with $\alpha = 4.4$ and $\beta = 1$. The solid lines (a) and (b) in Panel C represent the gamma functions with $\alpha = 60$ and $\beta = 0.14$, and $\alpha = 4.4$ and $\beta = 1$, respectively. The solid line (c) is the convoluted distribution curve made from the lines (a) and (b). The inserted illustrations in the panel schematically show a possible molecular aggregate consistent with the distribution. The complex contains longer rods as the minor species, which is considered to be made from more than two s-SPG chains, whereas, the renatured schizophyllan is mainly made from three s-SPG chains. The different distribution between (B) and (C) evidences the complex formation.

Table 1. Molecular weight and its distribution estimated from the AFM images

Sample	Number average L/nm	$M_n/10^4$	$M_w/10^4$	M_w/M_n
t-SPG (from AFM)	215	46.7	55.8	1.2
s-SPG(from AFM)	220	47.7	59.3	1.2
s-SPG/poly(C) (from AFM)	262	56.9	72.7	1.3
t-SPG (from GPC)	—	36.0	45.0	1.3

Therefore, the actual diameter of the t-SPG sample is ~2–6 nm, which is larger than the crystallographic data (2.6 nm).[11,12] It is interesting that we observe the image

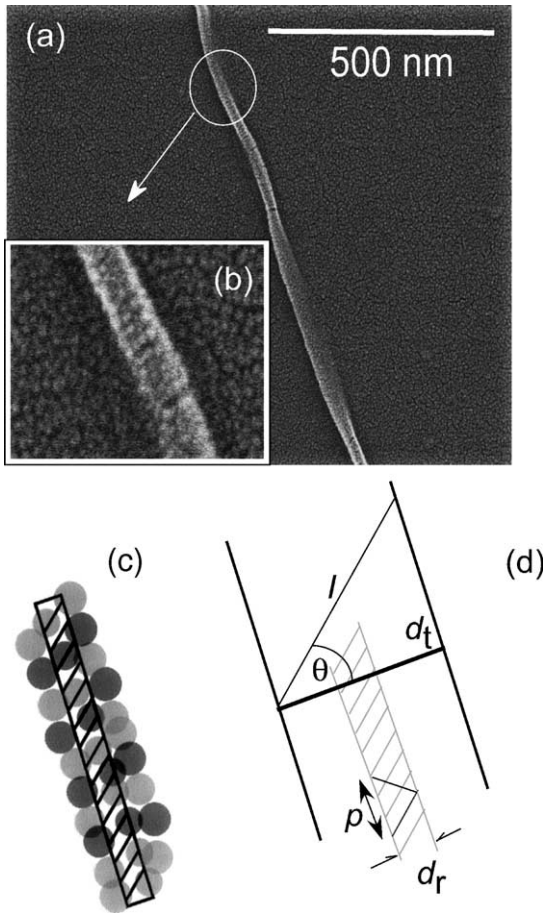

Figure 5. A SEM image of the triple helix of schizophyllan (a) and a magnified image (b). Panel c is a model that shows the platinum grains are arrayed using the molecular surface as the template, and Panel d presents the definitions of the lengths and angles. The incremental angle θ is determined by $\theta = \cos^{-1}(I/d_t)$, where I and d_t are the length of the grain array and the diameter of the image, respectively. The definitions of p and d_r are described in the text.

that, the platinum grains attached onto the sample, array regularly with a fixed value of the inclination angle relative to the rod axis. Through examination of several samples, we confirmed that the helical pattern is always right handed, being consistent with the expected helicity of t-SPG. The essential process acquired to obtain such a pattern is metal shadowing (see the Experimental section). The averaged inclination angle (θ) was evaluated to be 20–25° from Figure 5, as well as from other images taken under the same conditions, using the equation of $\theta = \cos^{-1}(I/d_t)$, where I is the length of the grain array (see Panel d in Fig. 5). Thus the value of θ so obtained can be related to the helix pitch (p) and the diameter of the real molecule (d_r) with the following equation:

$$p = 2d_r \tan(\theta). \quad (1)$$

Using Eq. 1, p can be evaluated to be between 2.0 and 2.4 nm, where d_r is the diameter of the real molecule; therefore, we use the crystallographic data: $d_r = 2.6$ nm.

This value of p is relatively larger than the crystallographic pitch (1.8 ± 0.1 nm).[12] By taking account of ambiguity involved in the present evaluation of p, the value obtained from AFM can be considered to be in the same order as that of the crystallographic data. All the above discussions on the SEM observations conclude that the array of platinum grains reflects the helicity of the triple helix of schizophyllan.

The finest resolution of the SEM observation is usually only a few nm, which is determined by the size of the metal grain. In fact, the platinum grain size in our picture ranges ~4–5 nm. Therefore, one might consider that it is strange to be able to achieve 2-nm resolution in our SEM observation, that is, to be able to observe the 1.8 nm pitch of t-SPG. We evaluated the pitch not directly but through the inclination of the metal-grain array using Eq. 1. It is true that the helical image in the SEM picture is incontrovertible (see Panel b in Fig. 5) and that we frequently observe such a pattern. We presume that when we coat the sample with platinum grains by shadowing, they are caught by the side chains of the schizophyllan, which should stick out from the molecules. In other words, the platinum grains array on the surface of t-SPG using the molecular helicity as a template (see Panel c in Fig. 5).

Figure 6 shows an image from the renatured s-SPG. This image exhibits a rod-like architecture, and the surface also shows a helical pattern. Although the helical resolution is poorer than that of t-SPG, we can confirm that the value of p is in the range of 2–3 nm. Although not shown, sometimes we observed rings in the SEM images, which is consistent with the AFM results.

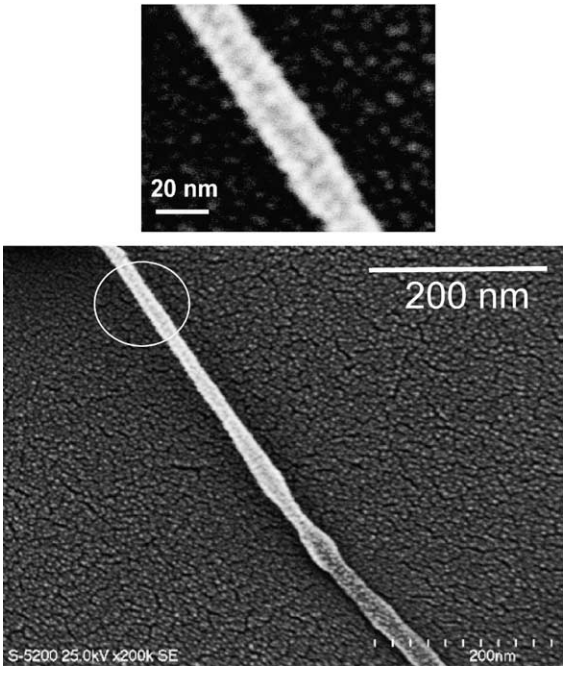

Figure 6. SEM images of the renatured schizophyllan showing the rod architecture and its magnification.

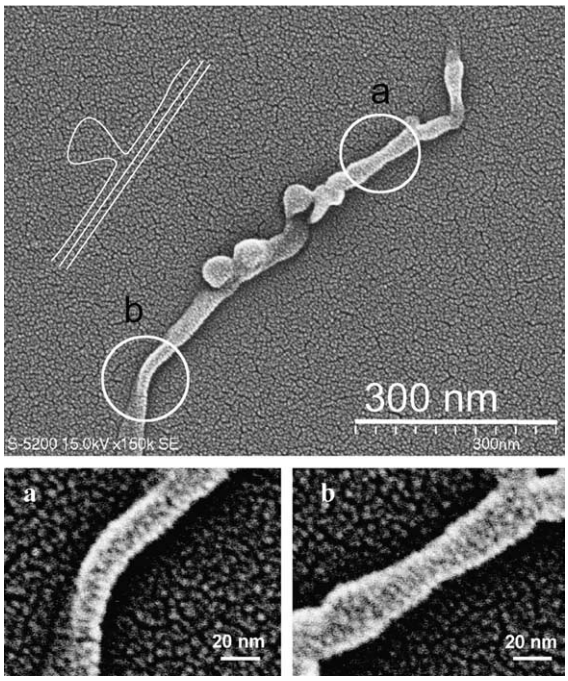

Figure 7. SEM images of the stoichiometric poly(C)/s-SPG complex. The upper image shows small bumps observed for the complex and a model for this architecture, and the lower images show magnification of the circled part of the image.

The stoichiometric complex of poly(C) and s-SPG shows somehow different features from that of the renatured s-SPG. Rings were less abundant than in the renatured sample, similar to the AFM observation. Instead of linear strands, small bumps were frequently observed on the rod-like images, as shown in Figure 7. The bumps on the rods may correspond to a defect of the complex, as illustrated in the insert of the figure. When the image of the strand is magnified, the same helical pattern is observed. The calculated pitch approximately agrees with that for t-SPG, although there is a relatively large experimental error. This helix pattern and agreement of the pitch length suggest that the poly(C)/s-SPG complex forms a triple helix with the same parameters as that of the original t-SPG.

The resolution of the images in Figures 6 and 7 is not as good as that in Figure 5. This reason could be that the side chains in the renatured s-SPG or complex line up less perfectly than those in the original triple helix depicted in Figure 1b.

3. Conclusions

The AFM and SEM observations reveal that the complex between poly(C) and schizophyllan forms the same rod-like architecture as for the renatured s-SPG and t-SPG,

indicating that a rod-like aggregate is formed upon complexation. The SEM observations show the helical pattern on the rod surface only when the sample was shadowed. The pitch evaluated from the image is comparable with that of the crystallographic data for t-SPG. The present microscopic studies indicate that the complex is a helical structure similar to that of t-SPG.

4. Experimental

4.1. Materials and complexation

Taito Co. in Japan kindly supplied the triple helical schizophyllan sample (t-SPG). The weight-average molecular weight (M_w) and the molecular weight distribution (defined by M_w/M_n where M_n is the number-average molecular weight) for the t-SPG sample, determined with gel-permeation chromatography (GPC) by use of a HLC-8020 (TOSOH), were 4.6×10^5 and 1.2–1.3, respectively. M_w and the number of repeating units for the single chain of SPG (s-SPG), evaluated from the intrinsic viscosity measurement in Me_2SO,[3,4] were 1.5×10^5 and 231 (in terms of the number of main chain glucose, 690 units), respectively. Poly(C) with the number of base = 570 was purchased from Amersham Pharmacia. The complex was prepared by mixing poly(C)/water with s-SPG/Me_2SO solutions, and then the solution was dialyzed for 48 h to remove Me_2SO. The complex solution was diluted to less than 2.6×10^{-3}–1×10^{-4} wt% and ultrasonicated for 5 min.

4.2. Electron microscopy observations

Dilute solutions of the original (natural) schizophyllan (t-SPG), renatured s-SPG, and poly(C)/s-SPG complex were cast onto freshly cleared mica, and the cast films were allowed to stand in clean air at room temperature in order to evaporate the solvent. The films were imaged by AFM (TopoMetrix) operating in a noncontact mode at room temperature, using a Si_3N_4 pyramidal tip (Cantilever Ultrasharp™ Silicium Cantilever). Field emission scanning electron microscopy (FE-SEM) was conducted with a Hitachi S-5200 instrument at an acceleration voltage of 15–25 kV. For the SEM observation, some of the metal-coated mica samples were initially frozen with liquid nitrogen for 5 min and then dried in vacuum. This freeze-drying procedure did not create any significant artificial effects. The mica samples were attached on the SEM specimen, and the specimen was positioned horizontally to the heated tungsten filament in the vacuum chamber. The specimen was coated with platinum for 5 s from both sides and subsequently coated vertically for 70 s, using a Hitachi E-1030 ion sputter (15 mA, 10 Pa). This shadowing technique was necessary in order to observe the molecules; otherwise, the molecules seemed to be buried in the platinum grains. The thickness of the metal coat was evaluated from the coating time and the current.

4.3. Statistical analysis of the AFM images

We measured the contour length (L) of the rod-like images in the AFM pictures using a flexible ruler. In the measurements we omitted dots, circles, and aggregates by judging width and shape. Since the distribution of L versus population obtained from AFM images had a similar shape with that of the gamma distribution, we fitted the histogram using the following equation:

$$f(x) = \frac{x^{\alpha-1}\exp\left(-\frac{x}{\beta}\right)}{\beta^{\alpha}\Gamma(\alpha)}, \qquad (2)$$

where $f(x)$, α, β, and $\Gamma(\alpha)$ are the probability distribution function, the shape parameter, scale parameter, and the gamma function, respectively. The case where $\beta = 1$ is called the standard gamma distribution. For convenience, we defined $x = L/40$ and obtained the most matched curve for the data by regression analysis. To convert L to the molecular weight, the molar mass per unit contour length (M_L) of the schizophyllan triple helix was assumed to be 2170 nm^{-1} (according to Kashiwagi et al.[25]), and the equation of $L = M/M_L$ was used.

Acknowledgements

This work has been financially supported by SORST and PRESTO program of the Japan Science and Technology Corporation. The present SEM work was carried out at Instrumentation Center at the University of Kitakyushu.

References

1. Mizu, M.; Koumoto, K.; Kimura, T.; Sakurai, K.; Shinkai, S. *Polymer J.* **2003**, *35*, 714–720.
2. Takaba, K.; Ito, W.; Kojima, T.; Kawabata, S.; Misaki, A. *Carbohydr. Res.* **1981**, *89*, 121–135.
3. Norisuye, T.; Yanaki, T.; Fujita, H. *J. Polym. Sci. Polym. Phys. Ed.* **1980**, *18*, 547–558.
4. Yanaki, T.; Norisuye, T.; Fujita, H. *Macromolecules* **1980**, *13*, 1462–1466.
5. Sato, T.; Sakurai, K.; Norisuye, T.; Fujita, H. *Polym. J.* **1983**, *15*, 87–96.
6. Mclntire, T. M.; Brant, D. A. *J. Am. Chem. Soc.* **1998**, *120*, 6909–6919.
7. Young, S. H.; Dong, W. J. *J. Biol. Chem.* **2000**, *275*, 11874–11879.
8. Sakurai, K.; Shinkai, S. *J. Am. Chem. Soc.* **2000**, *122*, 4520–4521.
9. Sakurai, K.; Mizu, M.; Shinkai, S. *Biomacromolecules* **2001**, *2*, 641–650.

10. Sakurai, K.; Shinkai, S. *J. Inclusion Phenom.* **2001**, *41*, 173–178.
11. Deslandes, Y.; Marchessault, R. H.; Sarko, A. *Macromolecules* **1980**, *13*, 1466–1471.
12. Bluhm, T. L.; Deslandes, Y.; Marchessault, R. H.; Pérez, S.; Rinaudo, M. *Carbohydr. Res.* **1982**, *100*, 117–130.
13. Saenger, W. *Principles of Nucleic Acid Structure*; Springer: New York, 1984; Chapter 13.
14. Merkel, R. *Phys. Rep.* **2001**, *346*, 343–385.
15. Hansma, H. G. *Biophys. J.* **1995**, *68*, 1672–1677.
16. Hansma, H. G.; Laney, D. E.; Bezanilla, M.; Sinsheimer, R. L.; Hansma, P. K. *Biophys. J.* **1995**, *68*, 1672–1677.
17. Mou, J.; Czajikowsky, D. M.; Yiyi, Z.; Zhifeng, S. *FEBS Lett.* **1995**, *371*, 279–282.
18. Camesano, T. A.; Wilkinson, K. J. *Biomacromolecules* **2001**, *2*, 1184–1191.
19. Kirby, A. R.; Gunning, A. P.; Ridout, M. J. *Biophys. J.* **1995**, *68*, 358–362.
20. Morris, V. J.; Mackie, A. R.; Wilde, P. J.; Kirby, A. R.; Mills, E. C. N.; Gunning, P. A. *Leben.-Wissen. Technol.* **2001**, *34*, 3–10.
21. McIntire, T. M.; Brant, D. A. *Int. J. Biol. Macromol.* **1999**, *26*, 303–310.
22. Stokke, B. T.; Elgsaeter, A.; Kitamura, S. *Polym. Gel Networks* **1994**, *2*, 173–190.
23. Kunitake, M.; Ohira, A. *Kobunshi* **2002**, *51*, 240–244; *Chem. Abstr.* **2002**, *137*, 310456.
24. Tasker, S.; Matthijs, G.; Davies, M. C.; Roberts, C. J.; Schacht, E. H.; Tendler, S. J. B. *Langmuir* **1996**, *12*, 6436–6442.
25. Kashiwagi, Y.; Norisuye, T.; Fujita, H. *Macromolecules* **1981**, *14*, 1220–1225.